Historic England

Remote Sensing

Wealden Glass Project, Archaeomagnetic Dating Report, April 2014

Paul Linford

Discovery, Innovation and Science in the Historic Environment

Research Report Series no. 12-2016

Research Report Series 12-2016

WEALDEN GLASS PROJECT

ARCHAEOMAGNETIC DATING REPORT, APRIL 2014

Paul Linford

NGR: TQ 008 237 and SU 928 336

ISSN 2059-4453 (Online)

For more information write to Res.reports@HistoricEngland.org.uk
or mail: Historic England, Fort Cumberland, Fort Cumberland Road, Eastney, Portsmouth PO4 9LD

SUMMARY

Fired clay remains from two sites associated with the medieval and post-medieval glassmaking industry in the Sussex and Surrey Weald were sampled for archaeomagnetic analysis. At Glasshouse Lane a fired clay surface associated with the glassmaking remains produced an archaeomagnetic date of AD 1555 – 1650 at 95% confidence, while at Imbhams Farm it was possible to sample the clay lining of the furnace itself yielding a date of AD 1515 – 1565 at 95% confidence. A summary of key information for archaeomagnetic database compilers can be found on page 10.

CONTRIBUTORS

The author was assisted with on-site sampling by Zoë Edwards at Glasshouse Lane during her Historic Environment Placement with the Geophysics Team and at Imbhams Farm by Aimée Ramgolam who had volunteered to help Surrey County Archaeological Unit (SCAU) with the excavation.

ACKNOWLEDGEMENTS

The author is grateful to the land owners and tenant farmers – Leconfield Estates and Roger Lywood at Glasshouse Lane and Margaret Barlow and Simon Carter at Imbhams Farm – for allowing archaeological investigations to take place. Thanks are also extended to Tom Munnery and Rob Poulton of the SCAU for help facilitating the archaeomagnetic sampling and providing useful background information and colleague Andy Payne for helping Zoë carry out the geophysical surveys.

ARCHIVE LOCATION

Fort Cumberland, Portsmouth.

DATES OF SAMPLING

Glasshouse Lane was visited to carry out archaeomagnetic sampling on the 28th March 2014 and Imbhams Farm on the 11th April 2014. The cover image shows a view of the Glasshouse Lane excavation looking SW.

CONTACT DETAILS

Paul Linford, Geophysics Team (Remote Sensing), Historic England, Fort Cumberland, Fort Cumberland Road, Eastney, Portsmouth PO4 9LD.
Tel: 02392 856749. Email: paul.linford@HistoricEngland.org.uk

CONTENTS

INTRODUCTION

The Wealden Glass project is a collaboration between Historic England and the Surrey County Archaeological Unit (SCAU) to investigate the medieval and early post-medieval glassmaking industry in the Weald of Surrey and Sussex (Poulton and Dungworth 2008). The archaeological evidence for this industry is considered of national importance and has been the subject of a long history of investigation dating back almost a hundred years. Nevertheless, gaps remain in the knowledge base: many sites may still be unrecorded; the condition and exact location of others is uncertain; and the technological development of the industry over the period of its existence is not well understood.

An initial programme of desk based assessment identified 50 separate glassmaking sites and 19 of these were selected for field survey via topographic recording and magnetometer survey (SCAU 2011). From this work a shortlist of three sites was drawn up for excavation to recover artefactual evidence and fired material for archaeomagnetic dating. The first excavation at Lordings Farm uncovered evidence for glassmaking but no furnace remains despite promising anomalies being detected in the magnetometer survey (Munnery 2014). Hence, additional magnetometer survey was undertaken immediately prior to excavation at the other two sites, Glasshouse Land and Imbhams Farm, to maximise the chance of siting targeted trenches directly over furnace remains (Edwards 2014).

On excavation, both sites revealed furnace remains although the furnace structure appeared to have been removed at Glasshouse Lane. The sites are both situated on loamy clayey soils (NRSI Soilscapes mapping) overlying mudstones of the Weald Clay Formation (British Geological Survey (NERC) 2014). At Imbhams Farm this clay had been used as a lining in the furnace structure and at both sites areas of fired natural clay that had been exposed to heat from the glassmaking activities survived *in situ*. This material was sampled for archaeomagnetic analysis.

METHOD

Sample collection and preparation

Specimens were collected from both features using the disc method (see Appendix 1, section 1a) and orientated to true north using a gyro-theodolite. The archaeomagnetic feature prefix codes GHL and IM were used for those taken from Glasshouse Lane and Imbhams Farm respectively. All specimens were composed of the local Weald clay which had been reddened and baked hard by exposure to intense heat.

The distributions of sampling locations across the two features are shown in Figures 1 and 2 respectively. Seventeen specimens were recovered at Glasshouse Lane (GHL02, 08 and 09 proved too friable to extract) from context 116 and twenty-one from Imbhams Farm from contexts 104 and 116. All were subsequently consolidated in the laboratory using a Vinamul 40224 solution.

Measurement

The natural remanent magnetisation (NRM) measured in fired archaeological materials is assumed to be caused by thermoremanent magnetisation (TRM) created when the feature of which they were part was last heated. However, a secondary component acquired in later geomagnetic fields can also be present, caused by diagenesis or partial reheating. Additionally, the primary TRM may be overprinted by a viscous component, depending on the grain size distribution within the magnetic material. These secondary components are usually of lower stability than the primary TRM and can thus be removed by a process of partial demagnetisation.

Partial demagnetisation involves tumbling the specimen in an alternating magnetic field of fixed peak strength and measuring the resulting changes in its magnetisation. This AF demagnetisation removes the contribution of the more weakly magnetised particles (those with the lowest coercivities). The higher the peak field strength applied, the greater the proportion of the overall magnetisation removed. The procedure is repeated with increasing peak field strengths to build up a complete picture of the coercivity spectrum (or demagnetisation curve) of the specimen.

NRM measurements were first made for all specimens after which they were each demagnetised up to a maximum field strength of 100mT using successive incremental demagnetising fields of 1, 2.5, 5, 7.5, 10, 15, 20, 30, 50, 75 and 100 mT (see Tables 1 to 7 for Glasshouse Lane and 9 to 16 for Imbhams Farm). As indicated in the tables, in some cases the demagnetisation sequence was stopped before the 100 mT increment was reached when the remaining magnetisation became too weak to measure accurately.

Principal components analysis can be used to determine the various linear segments present within a demagnetisation curve (Kirshvinck 1980). In the ideal case, each linear segment will correspond with one of the magnetisation components described above. Linearity is determined using the Maximum Angular Deviation (MAD) statistic (see previous citation for definition). The smaller this statistic the better and, as a rule of thumb, sets of measurements with a MAD of <= 2.0° are considered acceptably linear. Once the linear segment corresponding to a specimen's primary magnetisation direction has been identified, its principal component is taken as the characteristic direction

of remanent magnetisation (ChRM). The results of this analysis for features GHL and IM are listed in Tables 8 and 17 respectively where the range of demagnetisation increments for which each specimen showed the highest linearity is recorded along with the corresponding MAD angle and calculated mean direction of magnetisation.

Calibration

Once the ChRM direction for each specimen has been determined, a mean ChRM direction can be calculated for the feature. Some specimens may be excluded from this calculation if their ChRM directions are so anomalous as to make them statistical outliers from the overall distribution. The mean direction is then adjusted according to the location of the feature relative to a notional central point in the UK (Meriden), so that it can be compared with standardised archaeomagnetic calibration data to produce a date of last firing for the feature.

Notes concerning the mean calculation and subsequent calibration can be found in sections 3 and 4 of Appendix 1. However, as explained under Results below, calibration of both features using the current standard UK calibration of Zananiri et al. (2007) produces date ranges that are not possible given archaeological and historical evidence. Fortunately, direct observations of the direction of the Earth's magnetic field began to be made in England during the 16th century (Malin and Bullard 1981) and the ChRM directions for the two Wealden furnaces are in close accord with the compiled data. Calibration was therefore performed by comparison with Malin and Bullard's data as transcribed into a reference curve by Clark, Tarling and Noël (1988).

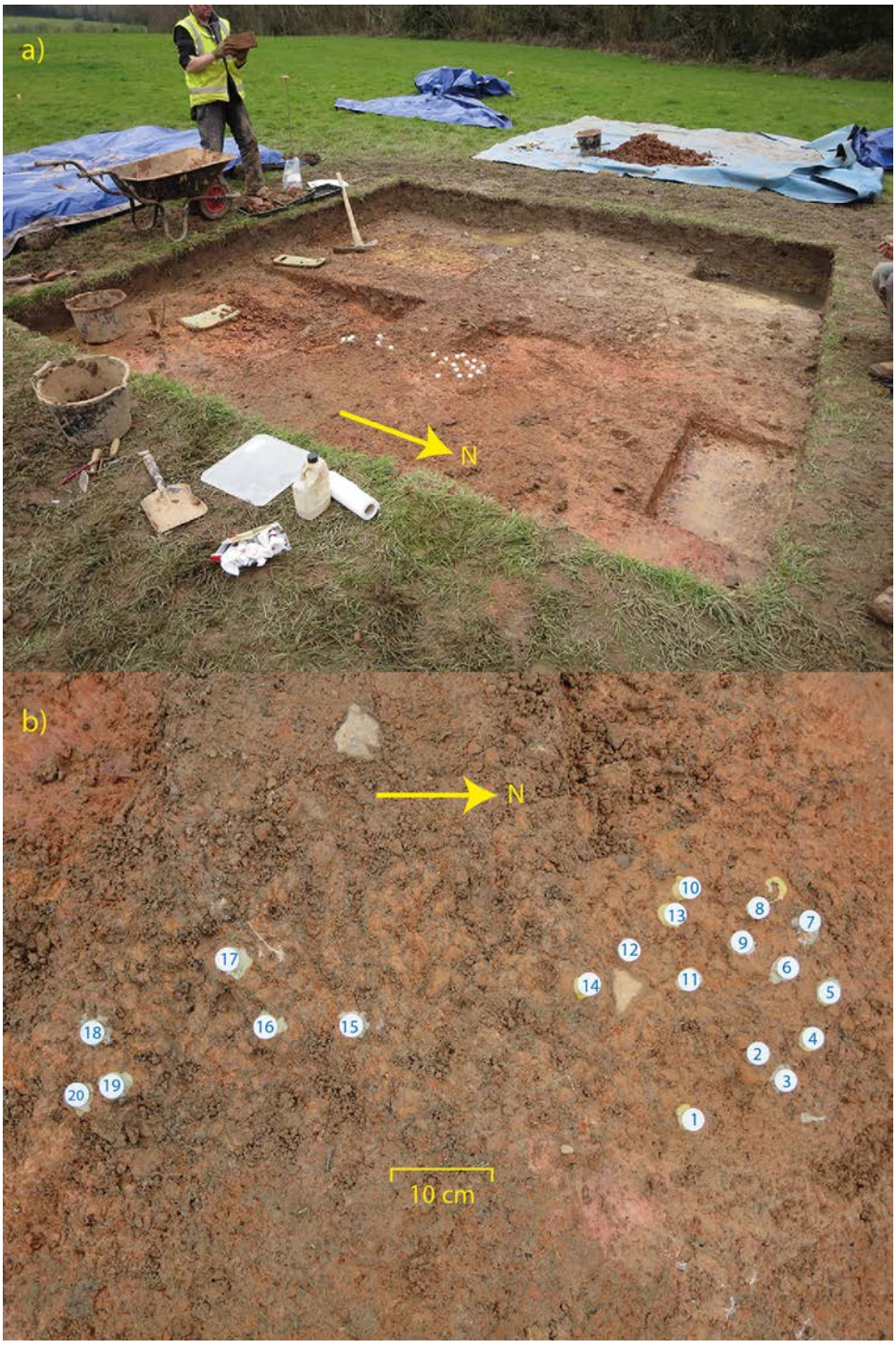

Figure 1a) the Glasshouse Lane excavation during archaeomagnetic sampling, the furnace pit is at the far (SW) corner; b) the fired clay surface showing distribution of specimens.

RESULTS

Glasshouse Lane (GHL, context 116)

As the archaeological assessment report (Munnery 2014) notes, the superstructure of the Glasshouse Lane furnace was found to have been removed, presumably to be re-used in another furnace elsewhere, leaving only a pit containing some disaggregated brick and stone in its basal fill. However, at Bagot's Park in Staffordshire where considerable effort was expended removing upstanding furnace remains in the 1960s to improve the land for agriculture, it was found that surviving fired natural clay from beneath the furnaces and working areas recorded a recoverable archaeomagnetic direction (Linford and Welch 2004). Specimens were therefore taken from an area of intensely fired natural Weald clay adjacent to the furnace pit (context 116, Figure 1).

On measurement the specimens' median destructive fields were found to be low, in the range of 10-14mT (see Table 1), and in all less than 3% of the NRM remained after demagnetisation in a 30mT field (Tables 2-7). This suggests that, while the clay surface was baked hard, it was not subjected to particularly intense heat, consistent with it being a natural clay surface lying beneath the furnace or annealing oven rather than part of the structure itself.

ChRM directions after demagnetisation are listed in Tables 1 and 8 and depicted in Figure 3b and five specimens were identified as outliers using Beck's (1983) test: GHL01, 03, 04, 07 and 17. All were close to the perimeter of the fired clay area and may either have been exposed to less intense heat resulting in incomplete magnetisation or possibly have been disturbed since the firing event. Figure 4 shows the demagnetisation curve of a rejected specimen, GHL03, which, when compared with more typical behaviour, such as that of GHL11 shown in Figure 5, can be seen to have a strong viscous component at lower coercivities. It appears this has overprinted the primary magnetisation which does not persist to the higher coercivities above 10mT that are less likely to be affected by viscous realignment. It is thus likely that the rejected samples were not exposed to sufficient heat in antiquity to acquire a stable remanent field direction. The mean ChRM direction of the remaining 12 specimens was calculated to be:

At site: Dec = 9.624^{o} Inc = 71.455^{o} α_{95} = 2.822^{o} k = 237.552
At Meriden: Dec = 10.153^{o} Inc = 72.289^{o}

When calibrated using the curve of Zananiri *et al.* (2007) and excluding prehistoric dates, the resulting date ranges at 95% confidence are AD 579 – 913 or AD 1660 – 1812. Unfortunately, both are incompatible with the archaeological evidence as the Wealden glassmaking industry is known to have begun in the medieval period and ended abruptly in 1615 when James I

prohibited the use of wood as fuel for glassmaking (see for instance Dodsworth 2003). However, as noted in Appendix 2, the Glasshouse Lane mean direction correlates closely with available calibration data for the 15th and 16th centuries, particularly the historical observations recorded towards the end of this period (Malin and Bullard 1981). It is therefore likely that there is a problem with the calibration curve for the early post-medieval period and, until this can be resolved, it is necessary to calibrate the Glasshouse Lane mean directly against the historical observations compiled by Malin and Bullard as transcribed into a reference curve by Clark, Tarling and Noël (1988). The calibration is depicted in Figure 6 and results in the date range of:

AD 1555 to 1650 at the 95% confidence level.

Figure 2a) the Imbhams Farm furnace during archaeomagnetic sampling; b and c) the fired clay surfaces for the W and E quadrants respectively showing distribution of specimens.

Imbhams Farm (IM, contexts 104 and 116)

Remains of the glassmaking furnace at Imbhams Farm were found *in situ* (Munnery 2014), formed of blocks of Upper Greensand lined with layers of local Weald clay. Two of the clay lining layers were sampled for archaeomagnetic dating (contexts 104 & 116, Figure 2).

On measurement the specimens' median destructive fields were found to be significantly higher than those from Glasshouse Lane, typically in the range 18-25mT with some as high as 33-34mT (Table 9), consistent with the material

having been exposed to intense heat as part of the furnace structure (Tables 10-16).

ChRM directions after demagnetisation are listed in Tables 9 and 17 and depicted in Figure 7b and four specimens were identified as outliers using Beck's (1983) test: IM01, 07, 08, 11 and 17. Typical demagnetisation behaviour is illustrated by specimen IM04 (Figure 8) which exhibits a weak viscous component at low coercivities but then maintains a persistent, primary magnetisation direction until the 50mT partial demagnetisation increment. Specimens 07 and 08 have similar demagnetisation curves (that for IM08 is shown in Figure 9) suggesting that their anomalous magnetisation directions are caused by disturbance since firing. Specimen IM11 has an unusually low MDF and appears not to have acquired a stable primary magnetisation (Figure 10). Presumably it was insulated from direct exposure to the furnace heat. Specimen IM17 (Figure 11) seems to have been well fired but its magnetisation direction changes considerably with increasing partial demagnetisation suggesting either movement during firing or the influence of other strongly magnetised parts of the furnace which cooled more quickly. Discounting these four, the mean ChRM direction of the remaining 17 specimens was calculated to be:

At site: Dec = 14.658° Inc = 67.965° α_{95} = 2.105° k = 288.100
At Meriden: Dec = 15.061° Inc = 68.769°

As with Glasshouse Lane, the Imbhams Farm mean ChRM direction is problematic when calibrated using the curve of Zananiri *et al.* (2007) with the resulting date range at 95% confidence being AD 666 – 1041 which is incompatible with the archaeological evidence. However, despite a slightly more easterly declination, the Imbhams mean direction is in good agreement with available calibration data for the 15th and 16th centuries (Appendix 2), particularly with that from around 1550. It has therefore also been calibrated directly against the historical observations compiled by Malin and Bullard as transcribed into a reference curve by Clark, Tarling and Noël (1988). The calibration is depicted in Figure 12 and results in the date range of:

AD 1515 to 1565 at the 95% confidence level.

CONCLUSIONS

Archaeomagnetic analysis demonstrates that the glassmaking furnace remains at both sites record stable thermoremanent directions allowing the last firing of each to be dated to the 16th century. The material sampled at Glasshouse Lane was less well fired than the furnace lining sampled at Imbhams Farm consistent

with the former being fired natural material that lay immediately beneath a furnace or annealing kiln which was subsequently removed. The lower firing temperature resulted in a less stable remanence direction being recorded which is reflected in the lower precision of the date for the Glasshouse Lane furnace.

The Imbhams Farm furnace dates to the earlier 16th century while Glasshouse Lane appears likely to date to the turn of the 17th century, not long before the cessation of glassmaking in the Weald brought about by James I's 1615 prohibition on the use of wood as a fuel. However, there was some evidence to suggest a subsequently robbed or dismantled third phase to the furnace at Imbhams Farm (Munnery 2014), so it is possible that the archaeomagnetic date does not relate to the last glassmaking activity at the site.

Calibration of the two ChRM directions using the UK archaeomagnetic calibration curve of Zananiri *et al.* (2007) resulted in date ranges that conflicted with the known archaeological and historical evidence. Examination of the calibration data for the 15th and 16th centuries (Appendix 2) suggests the explanation is that a refinement to the curve is needed to take account of direct observations of the Earth's magnetic field direction that began in this period.

ARCHAEOMAGNETIC DATE SUMMARY

Archaeomagnetic ID:	**GHL**
Feature:	**Fired clay surface, context 116**
Location:	**Longitude 0.56° W, Latitude 51.00° N**
Number of specimens (taken/used in mean):	**17/12**
AF Demagnetisation Applied:	**0-75mT (see text and tables)**
Distortion Correction Applied:	**None**
Declination (at Meriden):	**9.624° (10.153°)**
Inclination (at Meriden):	**71.455° (72.289°)**
Alpha-95:	**2.822°**
k:	**237.552**
Date range (95% confidence):	**AD 1555 to 1650**
Independent date estimate:	**Medieval to AD 1615**
Quality as calibration data:	**reasonable**

Archaeomagnetic ID:	**IM**
Feature:	**Glassmaking furnace, contexts 104 and 116**
Location:	**Longitude 0.676° W, Latitude 51.094° N**
Number of specimens (taken/used in mean):	**21/17**
AF Demagnetisation Applied:	**0-100mT (see text and tables)**
Distortion Correction Applied:	**None**
Declination (at Meriden):	**14.658° (15.061°)**
Inclination (at Meriden):	**67.965° (68.769°)**
Alpha-95:	**2.105°**
k:	**288.100**
Date range (95% confidence):	**AD 1515 to 1565**
Independent date estimate:	**Medieval to AD 1615**
Quality as calibration data:	**reasonable**

TABLES

Sample	NRM Measurements				After Partial Demagnetisation				
	Material	Dec^{o}	Inc^{o}	J(mAm^{-1})	AF(mT)	Dec^{o}	Inc^{o}	MDF(mT)	R
GHL01	Clay	-25.4	67.9	4862.7	75.0	-23.7	68.3	10.7	R
GHL03	Clay	140.1	-43.1	159.4	30.0	139.1	-44.4	12.6	R
GHL04	Clay	86.1	87.2	2096.8	75.0	120.5	88.4	10.9	R
GHL05	Clay	23.2	75.8	42.7	30.0	28.9	74.5	11.2	
GHL06	Clay	3.3	68.1	1279.9	50.0	6.1	67.5	10.6	
GHL07	Clay	45.8	54.4	456.4	30.0	47.5	55.2	10.8	R
GHL10	Clay	20.9	71.8	6546.8	50.0	23.6	70.4	11.5	
GHL11	Clay	12.9	73.2	3839.3	50.0	12.9	71.0	11.3	
GHL12	Clay	15.9	70.7	739.6	30.0	13.5	70.0	10.4	
GHL13	Clay	29.9	72.1	1769.8	50.0	30.5	70.3	10.7	
GHL14	Clay	11.3	73.4	8226.4	50.0	7.9	74.8	10.6	
GHL15	Clay	-1.7	71.9	9266.4	50.0	-4.7	71.2	13.5	
GHL16	Clay	-0.9	74.8	13666.0	50.0	-1.1	75.0	12.4	
GHL17	Clay	153.6	76.0	3309.2	50.0	161.9	75.8	14.7	R
GHL18	Clay	-3.8	69.4	2768.5	50.0	1.5	68.4	14.3	
GHL19	Clay	11.3	65.7	4150.6	50.0	11.7	66.0	13.1	
GHL20	Clay	-12.8	72.0	6148.3	50.0	-17.6	72.9	12.8	

Table 1: NRM measurements of samples and measurements after partial AF demagnetisation for feature GHL. J = magnitude of magnetisation vector; AF = peak alternating field strength of demagnetising field; R = sample rejected from mean calculation.

AF(mT)	GHL01			GHL03			GHL04		
	Dec^{o}	Inc^{o}	J(mAm^{-1})	Dec^{o}	Inc^{o}	J(mAm^{-1})	Dec^{o}	Inc^{o}	J(mAm^{-1})
0.0	-19.3	67.5	4794.3	138.0	-41.0	158.4	125.0	88.3	2100.2
1.0	-20.9	67.7	4802.1	138.3	-42.4	161.9	114.3	88.1	2093.5
2.5	-22.4	68.1	4694.3	138.3	-43.3	165.1	112.4	87.9	2055.3
5.0	-23.3	68.1	4249.9	139.5	-43.2	158.3	112.7	87.7	1841.9
7.5	-24.0	68.1	3404.0	140.3	-43.4	138.7	111.8	87.9	1555.8
10.0	-24.2	68.0	2618.5	141.0	-42.1	112.7	122.9	88.3	1168.0
15.0	-24.7	67.7	1000.0	143.8	-38.3	47.6	123.8	88.3	518.4
20.0	-28.5	68.5	364.0	148.8	-30.4	18.9	135.0	87.9	172.2
30.0	-28.7	71.5	108.9	158.4	13.6	4.7	-50.8	86.6	46.4
50.0	-52.2	65.0	66.8	-	-	-	154.2	82.8	34.3
75.0	-34.5	69.4	60.1	-	-	-	-152.7	83.0	27.8

Table 2: Incremental partial demagnetisation measurements for samples GHL01, GHL03 and GHL04.

AF(mT)	GHL05			GHL06			GHL07		
	Dec^{o}	Inc^{o}	J(mAm^{-1})	Dec^{o}	Inc^{o}	J(mAm^{-1})	Dec^{o}	Inc^{o}	J(mAm^{-1})
0.0	31.2	78.3	53.6	0.7	71.5	1247.2	47.5	56.7	451.4
1.0	28.4	76.9	54.1	1.8	70.9	1238.9	47.8	56.3	446.2
2.5	27.4	76.8	53.8	2.1	70.6	1214.8	47.4	56.0	435.2
5.0	28.5	77.3	50.2	2.3	70.0	1103.1	46.1	55.6	397.3
7.5	26.2	75.8	42.1	1.8	69.9	889.6	47.2	55.0	330.9
10.0	26.9	76.3	31.2	2.5	69.2	668.5	47.3	54.8	247.6
15.0	17.8	78.8	12.1	2.8	69.0	286.2	46.7	54.4	102.7
20.0	-74.1	86.5	6.5	-0.7	69.2	111.3	41.1	57.5	36.9
30.0	-65.5	87.1	4.1	-29.8	71.7	25.4	8.6	65.9	7.5
50.0	-	-	-	-70.9	68.5	13.0	-	-	-

Table 3: Incremental partial demagnetisation measurements for samples GHL05, GHL06 and GHL07.

AF(mT)	GHL10			GHL11			GHL12		
	Dec^{o}	Inc^{o}	J(mAm^{-1})	Dec^{o}	Inc^{o}	J(mAm^{-1})	Dec^{o}	Inc^{o}	J(mAm^{-1})
0.0	22.7	71.1	6475.6	9.8	73.5	3778.9	15.0	71.7	731.5
1.0	24.7	71.0	6422.9	13.8	73.3	3727.3	15.2	71.4	724.0
2.5	26.1	70.6	6293.6	15.1	72.7	3632.2	14.4	70.9	704.1
5.0	26.3	70.3	5728.8	15.8	72.3	3330.4	14.6	70.8	637.6
7.5	26.2	70.3	4832.5	15.5	72.2	2824.2	14.7	70.7	521.8
10.0	23.8	70.3	3904.7	12.0	72.3	2213.4	12.7	70.3	385.8
15.0	24.1	70.1	1705.6	12.6	71.3	977.8	8.6	70.4	161.9
20.0	24.6	70.0	628.0	11.9	72.0	350.5	1.3	70.5	65.3
30.0	25.6	73.0	118.6	9.1	74.2	76.2	-27.9	69.1	19.8
50.0	59.4	75.1	46.7	8.3	76.4	36.1	-	-	-

Table 4: Incremental partial demagnetisation measurements for samples GHL10, GHL11 and GHL12.

AF(mT)	GHL13			GHL14			GHL15		
	Dec^{o}	Inc^{o}	J(mAm^{-1})	Dec^{o}	Inc^{o}	J(mAm^{-1})	Dec^{o}	Inc^{o}	J(mAm^{-1})
0.0	29.8	72.6	1768.4	11.7	74.5	8307.2	-5.5	72.0	9207.0
1.0	29.1	72.3	1747.8	10.9	74.4	8231.0	-5.0	71.8	9150.6
2.5	28.0	71.7	1691.7	9.9	74.5	7945.2	-6.6	71.9	9041.6
5.0	28.6	71.3	1526.0	9.2	74.3	7285.2	-6.4	71.6	8608.2
7.5	29.1	70.6	1196.5	9.4	74.2	5932.0	-5.2	71.9	7792.5
10.0	29.2	70.5	958.5	10.0	74.0	4479.3	-4.2	71.3	6694.9
15.0	27.4	70.7	403.0	11.7	74.3	1927.3	-2.7	71.4	3690.9
20.0	23.7	71.2	192.4	10.4	74.6	769.3	-2.6	71.5	1520.1
30.0	15.9	72.2	91.4	10.0	75.9	243.2	-15.0	77.3	263.8
50.0	15.3	74.3	62.1	-1.7	78.5	134.4	170.4	72.3	55.5

Table 5: Incremental partial demagnetisation measurements for samples GHL13, GHL14 and GHL15.

AF(mT)	GHL16			GHL17			GHL18		
	Dec^{o}	Inc^{o}	J(mAm^{-1})	Dec^{o}	Inc^{o}	J(mAm^{-1})	Dec^{o}	Inc^{o}	J(mAm^{-1})
0.0	-1.3	75.1	13783.5	160.1	75.3	3335.5	-1.2	68.9	2848.9
1.0	-1.0	75.1	13683.9	160.4	75.3	3333.6	-2.6	68.8	2850.1
2.5	-0.7	75.1	13559.6	160.4	75.2	3307.5	-1.2	68.8	2819.3
5.0	0.0	75.2	12700.0	161.4	75.2	3199.9	-1.9	68.9	2694.6
7.5	0.0	75.0	11175.9	160.8	75.2	2944.9	-2.0	68.7	2480.3
10.0	0.3	75.1	9181.6	160.5	75.1	2606.4	-1.0	68.8	2155.6
15.0	1.7	75.0	4386.6	159.9	74.7	1607.9	0.5	68.4	1303.4
20.0	-1.2	75.1	1673.9	159.3	74.4	709.6	-1.3	68.1	535.7
30.0	-4.2	76.5	242.3	179.6	74.4	90.7	-13.6	68.8	81.7
50.0	-36.7	55.2	89.4	-88.0	49.6	20.0	-44.5	56.9	27.1

Table 6: Incremental partial demagnetisation measurements for samples GHL16, GHL17 and GHL18.

AF(mT)	GHL19			GHL20		
	Dec^o	Inc^o	J(mAm^{-1})	Dec^o	Inc^o	J(mAm^{-1})
0.0	13.1	66.6	4194.3	-18.1	72.7	6209.4
1.0	12.9	66.5	4188.1	-18.3	73.1	6177.0
2.5	12.5	66.4	4134.0	-19.7	72.8	6116.1
5.0	11.9	66.3	3941.0	-19.6	72.5	5798.5
7.5	-	-	-	-19.2	72.8	5130.9
10.0	12.1	65.8	2938.7	-17.6	72.7	4346.9
15.0	12.4	65.5	1579.8	-16.8	72.3	2110.3
20.0	13.5	64.9	578.6	-17.8	71.7	676.9
30.0	-7.3	63.9	72.3	-14.7	73.9	77.7
50.0	-47.8	75.7	29.1	-66.6	72.2	34.0

Table 7: Incremental partial demagnetisation measurements for samples GHL19 and GHL20.

Sample	Consistency						Linearity					
	Min	Max	N	MCI	Dec^o	Inc^o	Min	Max	N	MAD^o	Dec^o	Inc^o
GHL01	5.0	10.0	3	38.1	-23.8	68.1	7.5	15.0	3	0.1	-23.7	68.3
GHL03	2.5	7.5	3	9.6	139.4	-43.3	10.0	20.0	3	0.4	139.1	-44.4
GHL04	2.5	7.5	3	60.6	112.3	87.8	10.0	20.0	3	0.1	120.5	88.4
GHL05	1.0	5.0	3	21.2	28.1	77.0	7.5	15.0	3	0.5	28.9	74.5
GHL06	5.0	15.0	4	19.2	2.4	69.5	20.0	50.0	3	0.2	6.1	67.5
GHL07	7.5	15.0	3	24.2	47.1	54.7	7.5	15.0	3	0.2	47.5	55.2
GHL10	10.0	20.0	3	48.7	24.2	70.1	10.0	20.0	3	0.1	23.6	70.4
GHL11	2.5	7.5	3	24.8	15.5	72.4	15.0	30.0	3	0.1	12.9	71.0
GHL12	2.5	7.5	3	63.2	14.6	70.8	15.0	30.0	3	0.1	13.5	70.0
GHL13	7.5	15.0	3	24.7	28.6	70.6	10.0	20.0	3	0.0	30.5	70.3
GHL14	1.0	20.0	7	44.9	10.2	74.3	5.0	10.0	3	0.1	7.9	74.8
GHL15	10.0	20.0	3	33.0	-3.2	71.4	10.0	20.0	3	0.3	-4.7	71.2
GHL16	0.0	2.5	3	64.8	-1.0	75.1	7.5	15.0	3	0.1	-1.1	75.0
GHL17	1.0	10.0	5	73.3	160.7	75.2	7.5	15.0	3	0.1	161.9	75.8
GHL18	2.5	10.0	4	43.7	-1.5	68.8	15.0	30.0	3	0.2	1.5	68.4
GHL19	0.0	2.5	3	31.7	12.8	66.5	10.0	20.0	3	0.1	11.7	66.0
GHL20	2.5	7.5	3	37.2	-19.5	72.7	10.0	20.0	3	0.2	-17.6	72.9

Table 8: Assessment of the range of demagnetisation values over which each sample attained its maximum directional consistency and linearity for feature GHL. Min and Max indicate the range of demagnetisation values in mT over which each statistic was calculated and N is the number of consecutive measurements this represents. MCI is the maximum value of Tarling and Symons' consistency index (over 2 for a stable magnetisation). MAD is Kirshvink's maximum angular deviation (less than 2^o indicates linearity). In each case, declination and inclination values are for the mean direction calculated from all demagnetisation measurements in the range indicated.

Sample	NRM Measurements				After Partial Demagnetisation				
	Material	Dec^{o}	Inc^{o}	J(mAm^{-1})	AF(mT)	Dec^{o}	Inc^{o}	MDF(mT)	R
IM01	Clay	21.1	61.5	2826.9	100.0	18.0	61.4	33.3	
IM02	Clay	14.9	69.7	23654.5	100.0	4.7	68.5	23.7	
IM03	Clay	25.7	72.9	38859.7	100.0	25.7	72.2	19.4	
IM04	Clay	32.6	66.1	733.5	100.0	32.6	65.7	22.1	
IM05	Clay	21.1	69.9	3699.2	100.0	22.4	67.7	23.7	
IM06	Clay	11.8	63.3	442.5	100.0	18.9	66.4	25.4	
IM07	Clay	42.4	73.1	15500.6	100.0	43.4	74.6	34.0	R
IM08	Clay	49.2	75.2	8861.9	100.0	48.7	75.2	25.7	R
IM09	Clay	14.2	71.4	14543.5	75.0	11.6	70.1	16.7	
IM10	Clay	18.9	73.0	8137.9	75.0	20.4	71.4	18.7	
IM11	Clay	26.5	72.5	12170.2	100.0	39.4	73.6	9.1	R
IM12	Clay	4.6	72.7	487.7	100.0	7.5	68.6	26.9	
IM13	Clay	15.1	72.0	12072.7	100.0	10.9	72.3	29.2	
IM14	Clay	22.8	74.5	6472.2	100.0	19.2	71.9	23.3	
IM15	Clay	8.4	71.0	1324.9	100.0	3.7	70.2	25.4	
IM16	Clay	3.9	67.7	36434.9	100.0	0.1	69.4	18.4	
IM17	Clay	23.7	54.0	2978.8	100.0	29.2	53.9	26.9	R
IM18	Clay	5.1	63.8	9238.3	100.0	7.4	63.3	20.2	
IM19	Clay	17.0	66.9	15703.3	100.0	18.7	64.1	13.6	
IM20	Clay	12.3	67.9	11993.5	100.0	12.2	66.9	18.2	
IM21	Clay	10.6	60.1	253.6	100.0	13.7	61.8	19.3	

Table 9: NRM measurements of samples and measurements after partial AF demagnetisation for feature IM. J = magnitude of magnetisation vector; AF = peak alternating field strength of demagnetising field; R = sample rejected from mean calculation.

AF(mT)	IM01			IM02			IM03		
	Dec^{o}	Inc^{o}	J(mAm^{-1})	Dec^{o}	Inc^{o}	J(mAm^{-1})	Dec^{o}	Inc^{o}	J(mAm^{-1})
0.0	19.2	62.2	2864.6	13.8	68.8	23151.5	26.9	73.2	37239.2
1.0	19.9	62.3	2843.1	13.0	68.7	22948.1	25.6	73.1	37065.5
2.5	19.7	62.2	2836.3	13.1	68.7	22682.5	25.8	72.8	37219.8
5.0	19.4	61.9	2827.6	13.3	68.7	22156.1	24.5	72.7	36215.8
7.5	20.0	61.8	2788.3	12.8	68.7	21305.7	24.4	72.5	34441.3
10.0	19.6	61.9	2726.6	12.5	69.8	20416.9	23.9	72.4	31964.6
15.0	18.6	61.8	2560.3	11.9	69.7	17459.2	23.9	72.6	25178.8
20.0	18.6	61.7	2289.1	11.5	69.4	13912.8	24.6	72.3	17773.1
30.0	18.4	61.8	1586.5	10.5	69.3	7582.4	24.3	72.3	7383.9
50.0	20.1	62.5	640.5	11.3	71.9	3439.1	17.8	73.0	2851.4
75.0	14.5	58.7	483.4	25.8	69.2	2809.9	28.4	71.4	2318.4
100.0	15.5	62.2	418.6	10.8	70.3	2581.5	17.2	72.1	2186.6

Table 10: Incremental partial demagnetisation measurements for samples IM01, IM02 and IM03.

AF(mT)	IM04			IM05			IM06		
	Dec^{o}	Inc^{o}	J(mAm^{-1})	Dec^{o}	Inc^{o}	J(mAm^{-1})	Dec^{o}	Inc^{o}	J(mAm^{-1})
0.0	31.8	66.4	739.5	23.0	70.1	3700.6	13.9	64.6	445.6
1.0	31.6	66.0	740.8	22.9	70.1	3695.4	13.8	64.2	439.6
2.5	31.3	66.1	737.7	22.8	70.2	3674.0	13.3	64.3	441.0
5.0	31.7	66.2	716.0	22.5	70.0	3583.6	14.1	64.1	434.8
7.5	31.2	66.0	689.5	22.9	70.1	3460.7	13.2	64.1	424.4
10.0	31.5	65.8	656.5	22.7	69.9	3334.5	14.4	63.8	400.8
15.0	30.8	65.5	552.3	23.5	69.1	2851.3	14.0	63.5	363.9
20.0	31.5	65.7	419.4	23.0	69.4	2225.8	13.1	62.9	300.9
30.0	30.5	65.6	181.0	22.6	68.3	1205.4	11.7	61.6	156.8
50.0	23.0	65.1	49.0	23.9	69.5	447.5	10.2	59.2	43.8
75.0	15.0	65.2	35.2	22.5	69.8	290.9	13.3	56.8	21.3
100.0	19.2	63.4	32.3	25.6	66.7	249.5	9.7	54.3	18.5

Table 11: Incremental partial demagnetisation measurements for samples IM04, IM05 and IM06.

AF(mT)	IM07			IM08			IM09		
	Dec^{o}	Inc^{o}	J(mAm^{-1})	Dec^{o}	Inc^{o}	J(mAm^{-1})	Dec^{o}	Inc^{o}	J(mAm^{-1})
0.0	43.2	73.7	15521.5	49.9	75.0	7625.2	11.6	70.8	12494.1
1.0	43.7	73.5	15369.1	47.2	74.7	7544.3	11.7	70.6	12470.1
2.5	41.5	73.0	15282.3	46.8	74.6	7556.1	10.8	70.6	12487.4
5.0	42.8	73.3	15128.7	46.6	74.7	7460.2	13.0	70.2	11802.8
7.5	41.7	74.2	14547.8	47.2	74.9	7274.6	13.2	70.0	10920.4
10.0	42.3	74.3	14269.2	47.6	74.7	6978.3	13.7	69.8	9914.3
15.0	41.9	74.4	13312.3	47.6	74.6	6208.7	14.5	69.6	7031.3
20.0	43.1	74.4	12095.2	47.9	74.8	5004.3	16.0	69.5	4714.8
30.0	39.5	74.0	8841.94	47.3	74.3	2931.4	14.7	69.5	2192.3
50.0	40.6	73.8	3447.85	45.6	73.5	1189.5	8.7	69.4	1037.2
75.0	52.6	67.1	2181.96	39.9	74.9	704.7	13.8	68.4	895.9
100.0	38.1	68.6	2246.54	40.9	72.1	546.5	-	-	-

Table 12: Incremental partial demagnetisation measurements for samples IM07, IM08 and IM09.

AF(mT)	IM10			IM11			IM12		
	Dec^{o}	Inc^{o}	J(mAm^{-1})	Dec^{o}	Inc^{o}	J(mAm^{-1})	Dec^{o}	Inc^{o}	J(mAm^{-1})
0.0	17.7	72.6	7064.2	43.6	74.4	10219.4	4.3	68.3	640.7
1.0	18.3	72.8	7049.8	40.7	74.0	10074.1	5.1	68.0	646.4
2.5	19.3	72.1	6999.9	38.7	73.7	9641.2	4.8	67.9	647.1
5.0	17.0	71.9	6785.6	39.1	73.4	8451.8	5.3	67.8	642.2
7.5	15.7	72.2	6333.3	38.5	73.1	6341.0	5.3	67.5	628.5
10.0	18.3	72.5	5807.2	38.4	72.9	4381.4	6.0	67.3	608.6
15.0	18.0	71.8	4438.5	36.6	71.9	1802.4	5.9	67.1	553.7
20.0	18.5	71.3	3222.0	32.0	72.0	725.2	5.5	66.8	448.0
30.0	15.6	71.0	1623.4	34.5	67.7	339.7	4.4	66.1	264.1
50.0	12.6	71.1	747.7	30.8	69.9	252.9	4.3	66.4	80.5
75.0	12.2	71.8	627.5	6.3	66.9	226.2	-0.8	64.1	39.2
100.0	-	-	-	15.8	72.4	209.2	-2.8	61.5	25.9

Table 13: Incremental partial demagnetisation measurements for samples IM10, IM11 and IM12.

AF(mT)	IM13			IM14			IM15		
	Dec^{o}	Inc^{o}	J(mAm^{-1})	Dec^{o}	Inc^{o}	J(mAm^{-1})	Dec^{o}	Inc^{o}	J(mAm^{-1})
0.0	14.5	71.0	11743.2	15.4	73.3	6344.7	5.5	70.7	1275.4
1.0	14.7	70.7	11709.0	15.8	73.0	6316.5	5.4	70.7	1273.1
2.5	14.4	71.0	11666.3	15.5	72.9	6281.3	5.2	70.7	1264.4
5.0	13.5	70.6	11614.9	15.9	72.7	6198.7	5.7	70.2	1244.5
7.5	11.8	70.6	11357.1	17.0	72.5	5954.3	6.5	70.3	1183.2
10.0	11.3	70.7	10989.3	17.9	72.3	5652.0	5.0	70.3	1155.3
15.0	10.8	70.8	10061.3	18.8	72.2	4749.0	6.4	70.2	1015.5
20.0	10.5	70.5	8571.0	19.6	72.4	3759.5	2.7	69.9	841.3
30.0	10.1	71.2	5630.8	18.5	72.7	1971.9	4.0	69.8	467.6
50.0	8.7	69.8	2580.2	23.6	72.4	538.3	-	-	-
75.0	8.9	68.7	1732.4	14.6	70.9	312.1	-8.3	66.6	77.4
100.0	7.1	67.9	1409.7	24.9	71.5	246.7	-1.4	66.1	55.7

Table 14: Incremental partial demagnetisation measurements for samples IM13, IM14 and IM15.

AF(mT)	IM16			IM17			IM18		
	Dec^{o}	Inc^{o}	J(mAm^{-1})	Dec^{o}	Inc^{o}	J(mAm^{-1})	Dec^{o}	Inc^{o}	J(mAm^{-1})
0.0	0.4	70.4	40727.5	29.3	52.5	2910.2	7.5	64.4	9181.5
1.0	0.5	70.3	40710.4	28.6	52.0	2880.9	7.3	64.3	9114.3
2.5	1.2	69.5	40976.6	27.7	51.9	2853.5	7.1	64.2	9024.3
5.0	1.3	70.1	39587.0	27.7	51.4	2772.8	6.8	64.0	8821.8
7.5	2.3	69.1	37747.5	26.7	51.1	2686.1	6.1	63.8	8339.1
10.0	1.3	69.0	35329.7	26.4	50.9	2568.3	5.9	63.7	7788.1
15.0	1.7	68.7	26847.4	25.4	49.7	2276.0	6.6	63.3	6223.9
20.0	2.5	68.6	17311.6	25.1	48.9	1878.9	6.3	63.5	4643.5
30.0	2.1	69.2	5140.9	22.9	46.3	1264.3	5.2	63.3	2184.9
50.0	-28.1	63.3	613.1	16.4	39.2	559.5	6.2	61.4	756.0
75.0	44.3	70.3	309.6	13.8	39.7	358.3	7.5	62.6	499.3
100.0	-36.1	65.1	304.1	4.4	40.3	240.7	8.6	59.2	434.5

Table 15: Incremental partial demagnetisation measurements for samples IM16, IM17 and IM18.

AF(mT)	IM19			IM20			IM21		
	Dec^{o}	Inc^{o}	J(mAm^{-1})	Dec^{o}	Inc^{o}	J(mAm^{-1})	Dec^{o}	Inc^{o}	J(mAm^{-1})
0.0	18.9	66.6	15634.7	8.9	67.4	12210.8	8.2	60.5	260.5
1.0	18.9	66.4	15574.8	9.9	67.2	12161.6	8.8	60.1	261.1
2.5	18.8	65.7	15308.0	10.3	67.0	12064.0	8.9	60.0	261.2
5.0	19.8	65.4	14273.5	10.5	67.0	11632.7	9.1	59.5	255.2
7.5	19.2	65.1	12455.0	9.5	66.8	10816.8	9.6	59.4	241.7
10.0	18.9	64.6	10314.0	10.7	66.8	9874.9	9.4	59.4	225.4
15.0	18.6	64.2	6817.5	10.0	66.6	7534.3	10.4	59.4	177.7
20.0	18.3	64.5	4176.9	9.4	66.7	5307.6	9.7	58.9	122.8
30.0	18.3	64.4	2001.4	11.9	65.7	2283.8	10.6	60.1	58.7
50.0	14.2	63.8	1160.4	12.6	64.0	757.4	6.3	56.2	17.1
75.0	19.8	63.7	1002.9	20.6	69.0	551.3	-2.1	50.8	10.4
100.0	18.2	65.4	901.0	-2.7	66.8	483.1	-1.6	46.0	8.2

Table 16: Incremental partial demagnetisation measurements for samples IM19, IM20 and IM21.

Sample	Consistency						Linearity					
	Min	Max	N	MCI	Dec^o	Inc^o	Min	Max	N	MAD^o	Dec^o	Inc^o
IM01	15.0	30.0	3	154.2	18.5	61.8	20.0	50.0	3	0.2	18.0	61.4
IM02	1.0	5.0	3	114.0	13.1	68.7	1.0	5.0	3	0.0	4.7	68.5
IM03	7.5	30.0	5	93.3	24.2	72.4	20.0	50.0	3	0.3	25.7	72.2
IM04	1.0	7.5	4	59.3	31.4	66.1	20.0	50.0	3	0.1	32.6	65.7
IM05	0.0	7.5	5	89.8	22.8	70.1	30.0	75.0	3	0.3	22.4	67.7
IM06	1.0	7.5	4	38.7	13.6	64.2	10.0	20.0	3	0.1	18.9	66.4
IM07	7.5	15.0	3	66.7	42.0	74.3	10.0	50.0	5	0.8	43.4	74.6
IM08	10.0	20.0	3	91.0	47.7	74.7	20.0	50.0	3	0.2	48.7	75.2
IM09	15.0	30.0	3	42.2	15.1	69.5	10.0	20.0	3	0.1	11.6	70.1
IM10	30.0	75.0	3	28.7	13.5	71.3	20.0	50.0	3	0.3	20.4	71.4
IM11	5.0	10.0	3	25.8	38.7	73.1	7.5	15.0	3	0.1	39.4	73.6
IM12	1.0	5.0	3	45.9	5.1	67.9	10.0	20.0	3	0.2	7.5	68.6
IM13	10.0	20.0	3	49.2	10.9	70.7	30.0	75.0	3	0.2	10.9	72.3
IM14	10.0	30.0	4	46.5	18.7	72.4	15.0	30.0	3	0.4	19.2	71.9
IM15	0.0	2.5	3	99.1	5.4	70.7	20.0	100.0	4	0.5	3.7	70.2
IM16	7.5	30.0	5	48.2	2.0	68.9	10.0	20.0	3	0.3	0.1	69.4
IM17	2.5	10.0	4	14.3	27.1	51.3	15.0	30.0	3	0.6	29.2	53.9
IM18	7.5	30.0	5	45.8	6.0	63.5	15.0	30.0	3	0.3	7.4	63.3
IM19	15.0	30.0	3	72.0	18.4	64.4	15.0	30.0	3	0.3	18.7	64.1
IM20	2.5	20.0	6	50.2	10.1	66.8	10.0	20.0	3	0.4	12.2	66.9
IM21	5.0	10.0	3	50.4	9.4	59.4	30.0	75.0	3	0.6	13.7	61.8

Table 17: Assessment of the range of demagnetisation values over which each sample attained its maximum directional consistency and linearity for feature IM. Min and Max indicate the range of demagnetisation values in mT over which each statistic was calculated and N is the number of consecutive measurements this represents. MCI is the maximum value of Tarling and Symons' consistency index (over 2 for a stable magnetisation). MAD is Kirshvink's maximum angular deviation (less than 2^o indicates linearity). In each case, declination and inclination values are for the mean direction calculated from all demagnetisation measurements in the range indicated.

APPENDIX 1: STANDARD PROCEDURES FOR SAMPLING AND MEASUREMENT

The principles underlying the archaeomagnetic dating method have been described by Linford (2004) and the procedures employed are described in English Heritage (2006). These notes summarise the most important points.

1) Sampling

One of three sampling techniques is employed depending on the consistency of the material (Clark *et al.* 1988; English Heritage 2006):

a) **Consolidated materials:** Rock and fired clay specimens are collected by the disc method. Several small levelled plastic discs are glued to the feature, marked with an orientation line related to True North, then removed with a small piece of the material attached.
b) **Unconsolidated materials:** Sediments are collected by the tube method. Small pillars of the material are carved out from a prepared platform, then encapsulated in levelled plastic tubes using plaster of Paris. The orientation line is then marked on top of the plaster.
c) **Plastic materials:** Waterlogged clays and muds are sampled in a similar manner to method 1b) above; however, the levelled plastic tubes are pressed directly into the material to be sampled.

2) Physical Analysis

a) Magnetic remanences are measured using a slow speed spinner fluxgate magnetometer (Molyneux 1971; Tarling 1983, p84; Thompson and Oldfield 1986).
b) Partial demagnetisation is achieved using the alternating magnetic field method (Tarling 1983, p91; Thompson and Oldfield 1986, p59) to remove viscous magnetic components if necessary. Demagnetising fields are measured in millitesla (mT), figures quoted being for the peak value of the field.

3) Remanent Field Direction

a) The remanent field direction of a specimen is expressed as two angles, declination (Dec) and inclination (Inc), both quoted in degrees. Declination represents the bearing of the field relative to true north, angles to the east being positive; inclination represents the angle of dip of this field.

b) Aitken and Hawley (1971) have shown that the angle of inclination in measured specimens is likely to be distorted owing to magnetic refraction. The phenomenon is not well understood but is known to depend on the position the specimens occupied within the structure. The corrections recommended by Aitken and Hawley are applied, where appropriate, to measured inclinations, in keeping with the practice of Clark, Tarling and Noel (1988).
c) Individual remanent field directions are combined to produce the mean remanent field direction using the statistical method developed by R. A. Fisher (1953). The quantity α_{95}, "alpha-95", is quoted with mean field directions and is a measure of the precision of the determination (see Aitken 1990, p247). It is analogous to the standard error statistic for scalar quantities; hence the smaller its value, the better the precision of the date.
d) Some specimen field directions may be excluded from the mean calculation if they are considered statistical outliers. The test suggested by Beck (1983) is used to identify such outliers.
e) For the purposes of comparison with standardised UK calibration data, remanent field directions are adjusted to the values they would have had if the feature had been located at Meriden, a standard reference point. The adjustment is done using the method suggested by Noel (Tarling 1983, p116).

4) Calibration

a) Material less than 3000 years old is dated using the archaeomagnetic calibration curve compiled by Zananiri *et al.* (2007).
b) Older material is dated using the lake sediment data compiled by Thompson and Turner (Thompson and Turner 1979; Turner and Thompson 1981).
c) Dates are normally given at the 95% confidence level. However, the quality of the measurement and the estimated reliability of the calibration curve for the period in question are not taken into account, so this figure is only approximate. Owing to crossovers and contiguities in the curve, alternative dates are sometimes given. It may be possible to select the correct alternative using independent dating evidence.
d) As the thermoremanent effect is reset at each heating, all dates for fired material refer to the final heating.

APPENDIX 2: EVIDENCE FOR THE MAGNETIC FIELD DIRECTION IN THE C15TH -16TH

Table 18a lists good quality archaeomagnetic evidence for the period between 1400 and 1600 and 18b lists recorded historical observations which began during the 16th century.

18a) Archaeomagnetic evidence	Dec	Inc	α_{95}	Estimated date
9-10 The Tything, Worcester (Linford 2003)	6.1	59.8	1.2	Late medieval, predates 1701
Beeleigh Abbey, Essex (Linford 2002)	8.9	60.6	2.0	1400 to 1500
Hartfield, Sussex, Lower Parrock, 77 (Clark *et al.* 1988)	14.1	64.6	3.4	1520 to 1550
Little Birches, Wolseley (Linford 1993; Welch 1997)	11.4	66.6	1.7	1500 to 1600
Furnace 4, Bagot's Park, Staffordshire (Crossley 1967)	11.9	66.2	0.4	1550 to 1600
18b) Historical observations	Dec	Inc		Date
Unknown	(7.2)	(69.4)		1540
Unknown	(11.2)	(70.4)		1550
Unknown	(9.6)			1560
Unknown	(~4.5)			~1570
Diggs?	~11.3			~1570
Frobisher (dec), Norman (inc)	11.5	71.8		1576
Norman	11.3			~1580
Borough	11.3			1580
Borough	10.8			1581
Polter	10.6			1586
Unknown (dec), Wright (inc)	11.0	(72.0)		~1600
Unknown	(9.3)	(73.0)		1600
Wright		(73.0)		1610
Unknown (dec), Ridley (inc)	(6.2)	(72.5)		1612-13

Table 18a) Archaeomagnetic calibration evidence for the period between 1400 and 1600 compared with 1b) recorded historical observations compiled by Malin and Bullard (1981). Figures in braces in the latter indicate lower reliability.

Both types of evidence indicate the Earth's magnetic field had a fairly constant declination of about 11 degrees east of true north over most of the period and a steadily increasing inclination (or dip) angle. However, there is a slight discrepancy where the two overlap around 1550 with the archaeomagnetic evidence suggesting the inclination angles was ~3 degrees shallower than the values reported by contemporary observers.

The calibration curve of Zananiri *et al* (2007), which is based only on archaeomagnetic evidence, has inclination values in agreement with Table 18 throughout this period but sets the declination at around 4 degrees east – too westerly to match the Wealden Glass ChRM directions. As archaeomagnetic evidence is relatively scant for the two centuries in question, it is likely that the

fitting algorithm has been influenced by archaeomagnetic calibration evidence from times just before 1400 and just after 1600. In both cases the declination moves very rapidly towards the west but recalculation of the calibration curve incorporating the direct observations recorded by Malin and Bullard (1981) may help counterbalance this influence.

It may be noted that the Glasshouse Lane ChRM direction matches closely with observations around or just before 1600 while the Imbhams Farm direction is consistent with the evidence from around 1500 - 1550.

REFERENCES

Aitken, M J 1990 *Science-based dating in archaeology*, London, Longman.

Aitken, M J and Hawley, H N 1971 'Archaeomagnetism: evidence for refraction in kiln structures'. *Archaeometry*, **13**, 83-5.

Beck, M E, Jr. 1983 'Comment on `Determination of the angle of a Fisher distribution which will be exceeded with a given probability' by P. L. McFadden'. *Geophysical Journal of the Royal Astronomical Society*, **75**, 847-849.

British Geological Survey (NERC) 2014 OpenGeoscience, Geology of Britain, map viewer. Geological Survey of Great Britain 1974 1:50,000 Geological Map Series - Sheet 301, Haslemere. [web page]; http://www.bgs.ac.uk/data/mapViewers/home.html. [Accessed 15/03/2016].

Clark, A J, Tarling, D H and Noël, M 1988 'Developments in Archaeomagnetic Dating in Britain'. *Journal of Archaeological Science*, **15**, 645-667.

Crossley, D W 1967 'Glassmaking in Bagot's Park, Staffordshire, in the sixteenth century'. *Post-medieval Archaeology*, **1**, 44-83.

Dodsworth, R 2003 *Glass and Glassmaking*, Princes Risborough, Shire.

Edwards, Z 2014 *'Two Wealden glass furnaces, Surrey and West Sussex, report on geophysical surveys, March 2014'*. English Heritage Research Department Report **21/2014**.

English Heritage 2006 *Archaeomagnetic Dating: Guidelines on producing and interpreting archaeomagnetic dates*, Swindon, English Heritage.

Fisher, R A 1953 'Dispersion on a sphere'. *Proceedings of the Royal Society of London A*, **217**, 295-305.

Kirshvinck, J L 1980 'The least-squares line and plane and the analysis of paleomagentic data'. *Geophysical Journal of the Royal Astronomical Society*, **62**, 699-718.

Linford, P 1993 *'Archaeomagnetic Dating: Little Birches, Wolseley, Staffordshire'*. English Heritage AML Report (New Series) **63/1993**.

Linford, P 2002 *'Beeleigh Abbey, Maldon, Essex: Archaeomagnetic Dating Report 2002'*. English Heritage Research Report **108/2002**.

Linford, P 2003 *'9-10 The Tything, Worcester: Archaeomagnetic Dating Report 2003'*. English Heritage Research Report **5/2003**.

Linford, P 2004 'Archaeomagnetic Dating'. *Physics Education*, **39** (2), 145-154.

Linford, P and Welch, C M 2004 'Archaeomagnetic analysis of glassmaking sites at Bagot's Park in Staffordshire, England'. *Physics of The Earth and Planetary Interiors*, **147** (2-3), 209-221.

Malin, S R C and Bullard, E 1981 'Direction of the Earth's magnetic field at London 1570-1975'. *Philosophical Transactions of the Royal Society of London*, **A299**, 357-423.

Molyneux, L 1971 'A complete result magnetometer for measuring the remanent magnetization of rocks'. *Geophysical Journal of the Royal Astronomical Society*, **24**, 429-433.

Munnery, T 2014 *'Wealden Glass Project: Preliminary assessment of three sites excavated as part of the Wealden Glass Project'*. Surrey County Archaeological Unit Assessment Report.

Poulton, R and Dungworth, D 2008 *'The Wealden Glass Industry: A Project Design'*. English Heritage Project Design.

SCAU 2011 *'An Archaeological Survey of 19 Sites Associated with the Glass Industry of the Weald in Surrey and Sussex'*. Surrey County Archaeological Unit Report.

Tarling, D H 1983 *Palaeomagnetism: Principles and applications on geology, geophysics and archaeology*, London, Chapman and Hall.

Thompson, R and Oldfield, F 1986 *Environmental Magnetism*, London, Allen and Unwin.

Thompson, R and Turner, G M 1979 'British geomagnetic master curve 10,000-0 yr BP for dating European sediments'. *Geophys. Res. Letters*, **6**, 249-252.

Turner, G M and Thompson, R 1981 'Lake sediment record of the geomagnetic secular variation in Britain during Holocene times'. *Geophysical Journal of the Royal Astronomical Society*, **65**, 703-725.

Welch, C M 1997 'Glass-making in Wolseley, Staffordshire'. *Post-medieval Archaeology*, **31**, 1-60.

Zananiri, I, Batt, C M, Lanos, P, Tarling, D H and Linford, P 2007 'Archaeomagnetic secular variation in the UK during the past 4000 years and its application to archaeomagnetic dating'. *Physics of The Earth and Planetary Interiors*, **160** (2), 97-107.

a)

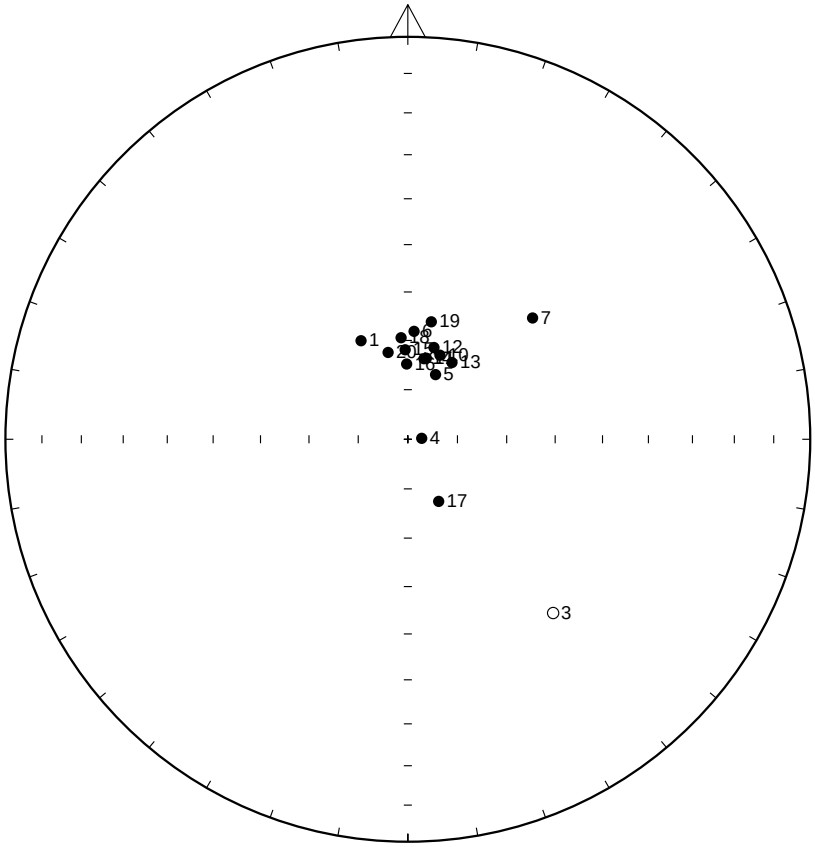

b)

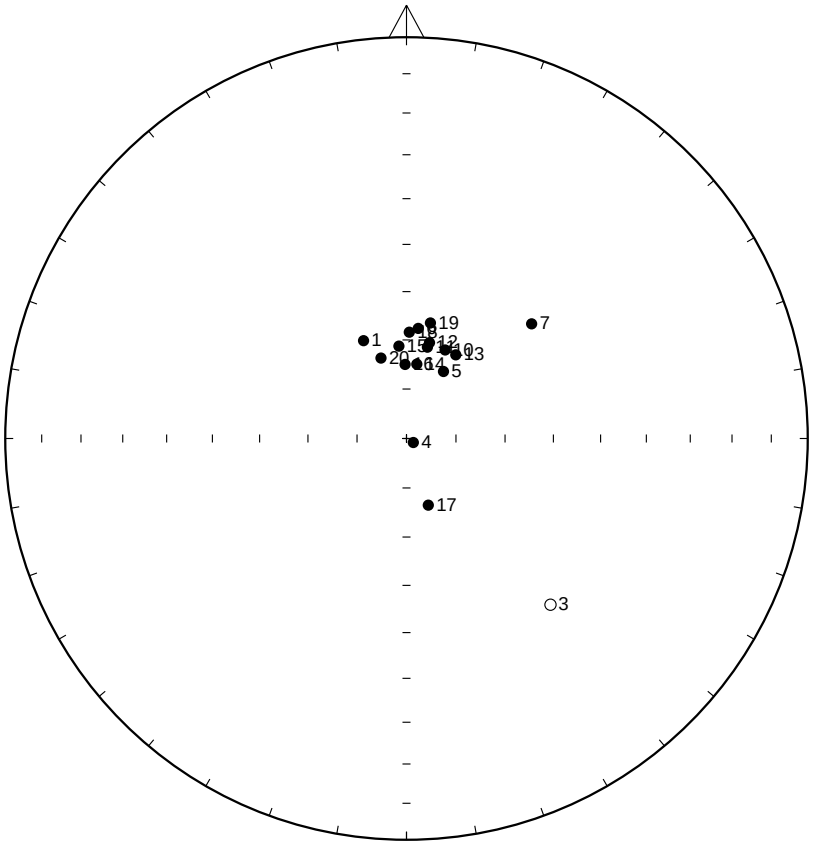

Figure 3: a) Distribution of specimen NRM directions from feature GHL represented as an equal area stereogram. In this projection declination increases clockwise with zero being at 12 o'clock while inclination increases from zero at the equator to 90 degrees in the centre of the projection. Open circles represent negative inclinations. b) Distribution of thermoremanent directions of magnetisation of the same specimens after partial AF demagnetisation.

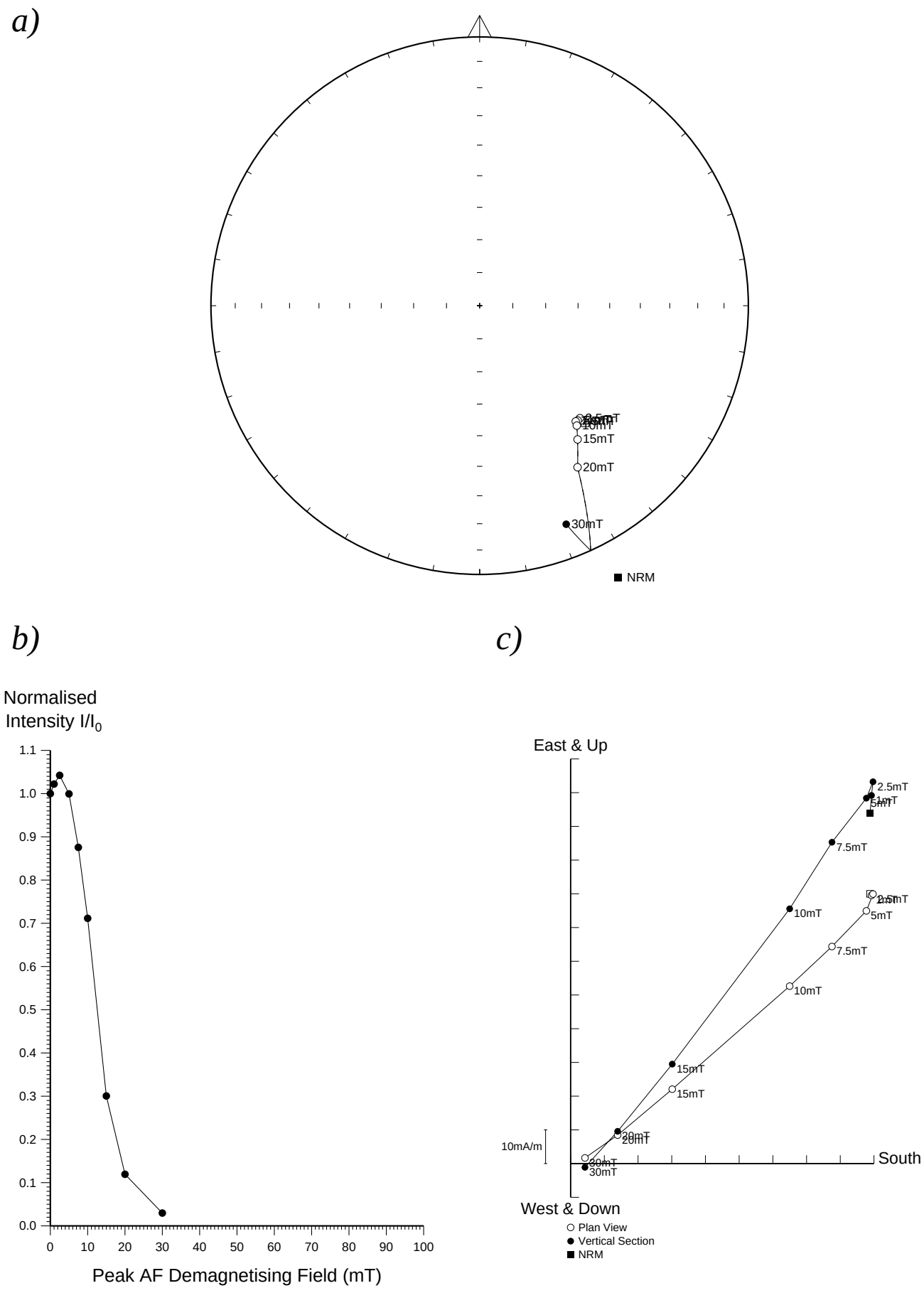

Figure 4: Stepwise AF demagnetisation of sample GHL03. Diagram a) depicts the variation of the remanent direction as an equal area stereogram (declination increases clockwise, while inclination increases from zero at the equator to 90 degrees at the centre of the projection); b) shows the normalised change in remanence intensity as a function of the demagnetising field; c) shows the changes in both direction and intensity as a vector endpoint projection.

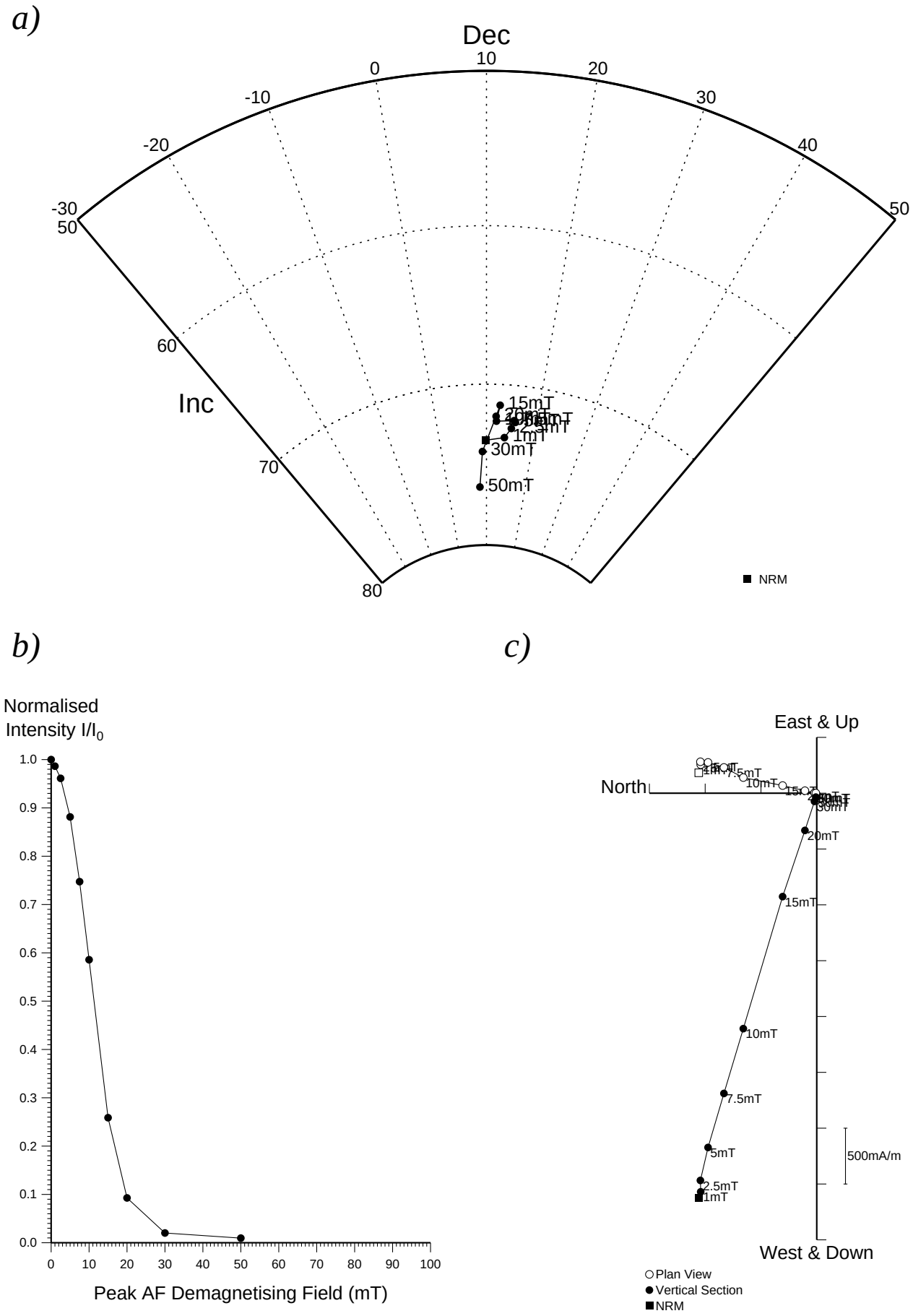

Figure 5: Stepwise AF demagnetisation of sample GHL11. Diagram a) depicts the variation of the remanent direction as an equal area stereogram; b) shows the normalised change in remanence intensity as a function of the demagnetising field; c) shows the changes in both direction and intensity as a vector endpoint projection.

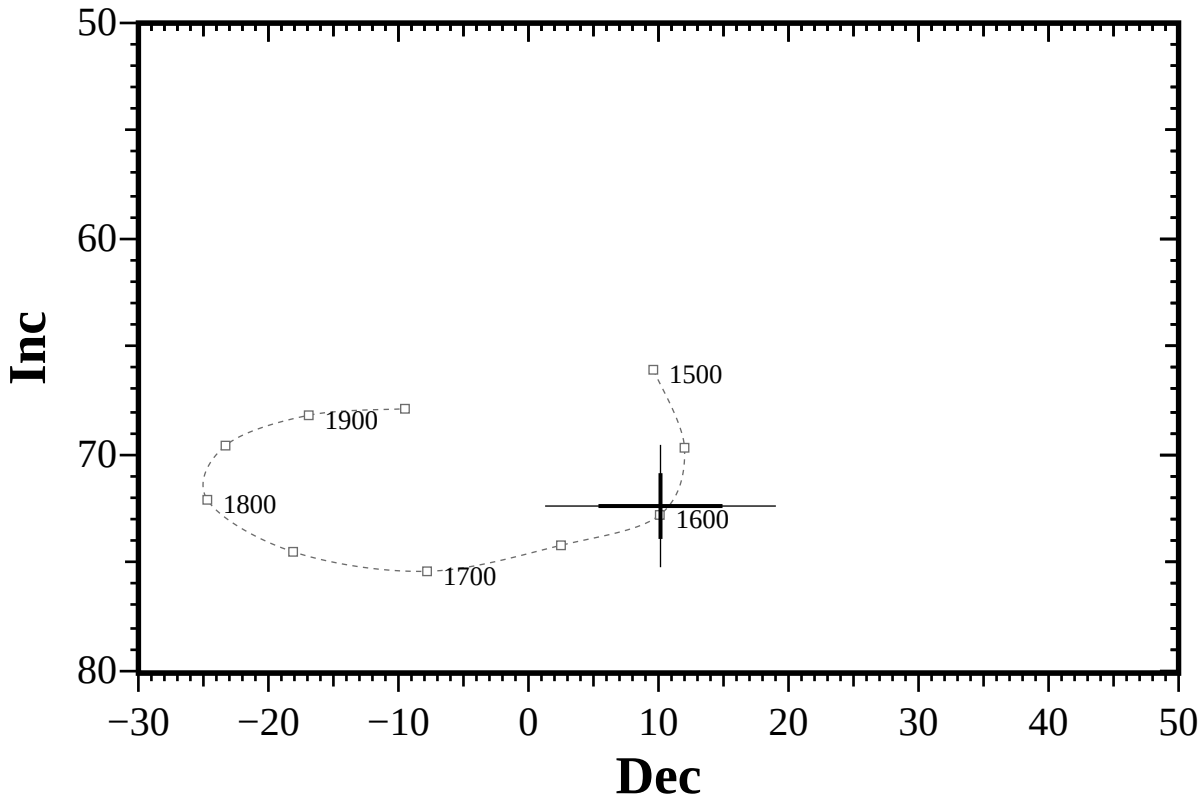

Figure 6: Comparison of the mean thermoremanent vector calculated from samples 05-06, 10-16 and 18-20 from feature GHL after partial demagnetisation with the UK master calibration curve. Thick error bar lines represent 63% confidence limits and narrow lines 95% confidence limits.

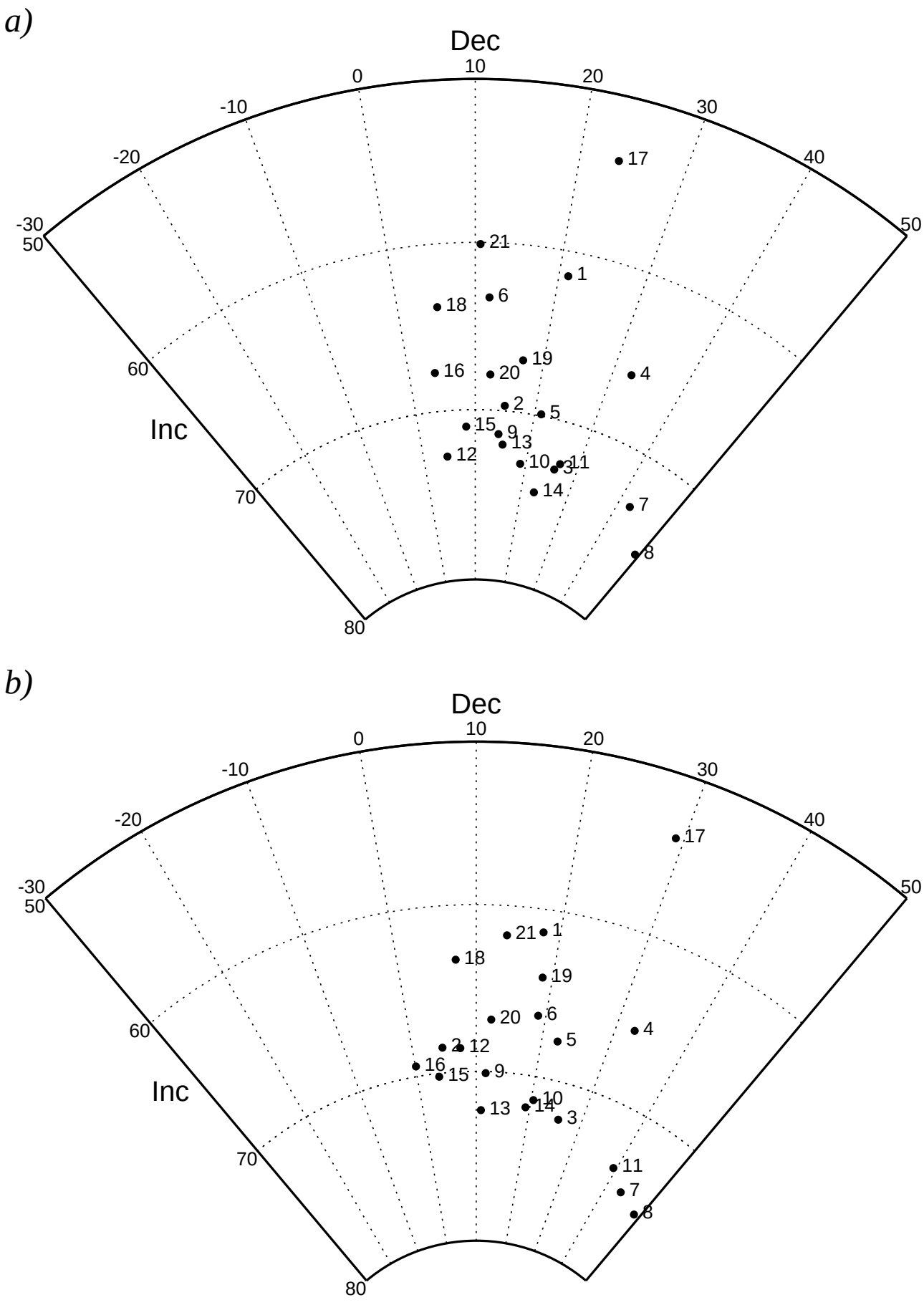

Figure 7: a) Distribution of specimen NRM directions from feature IM represented as an equal area stereogram. Open circles represent negative inclinations. b) Distribution of thermoremanent directions of magnetisation of the same specimens after partial AF demagnetisation.

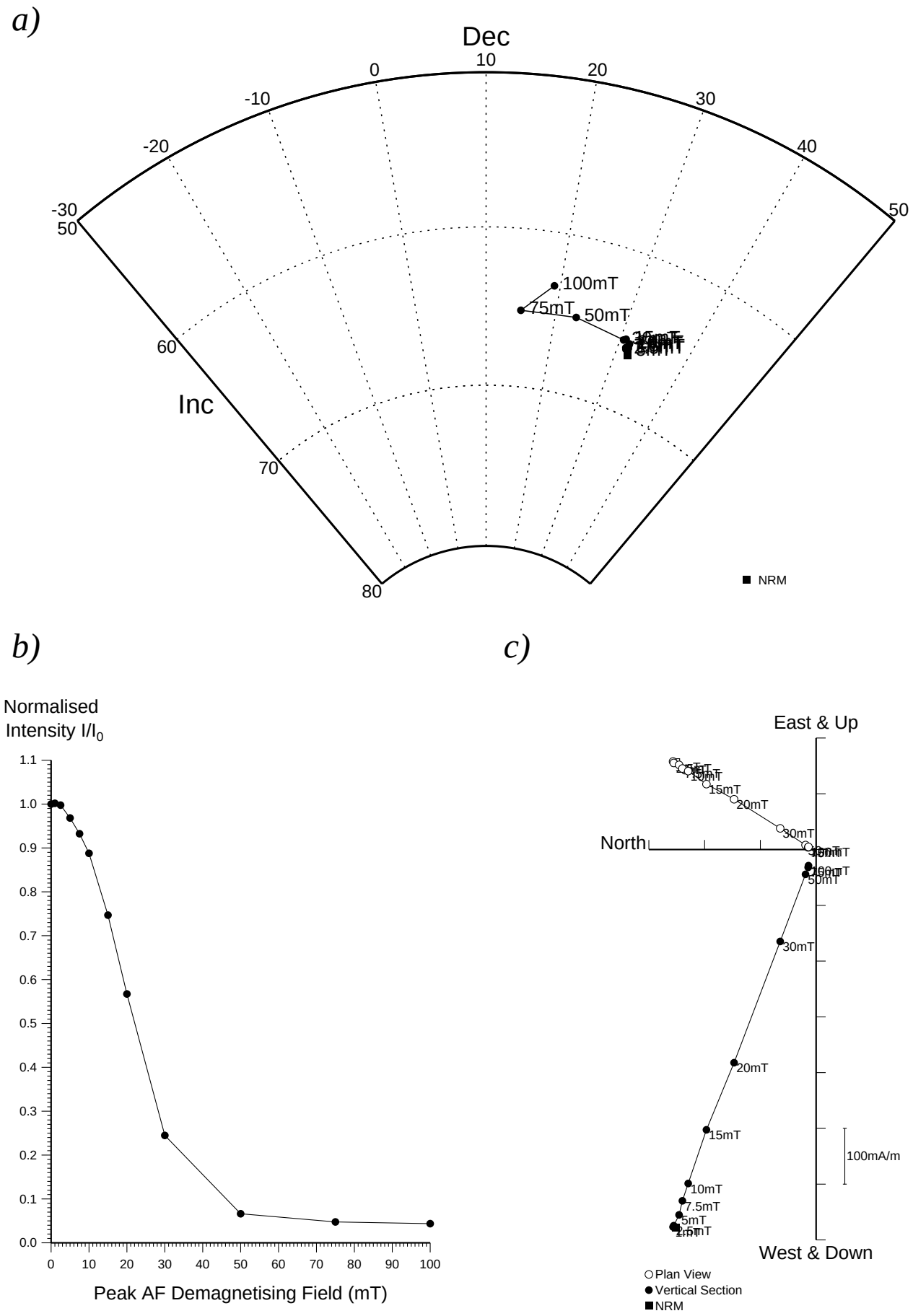

Figure 8: Stepwise AF demagnetisation of sample IM04. Diagram a) depicts the variation of the remanent direction as an equal area stereogram; b) shows the normalised change in remanence intensity as a function of the demagnetising field; c) shows the changes in both direction and intensity as a vector endpoint projection.

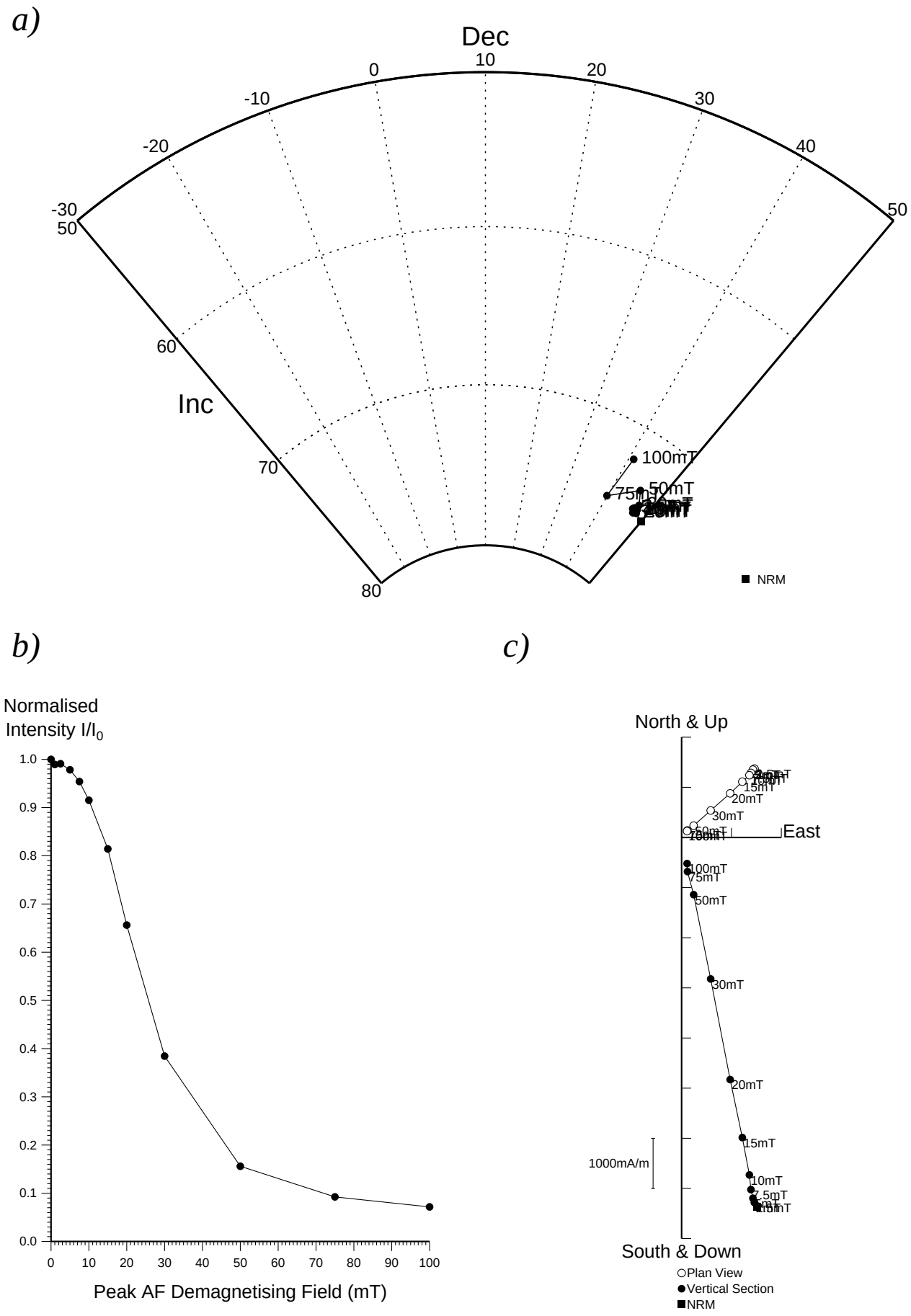

Figure 9: Stepwise AF demagnetisation of sample IM08. Diagram a) depicts the variation of the remanent direction as an equal area stereogram; b) shows the normalised change in remanence intensity as a function of the demagnetising field; c) shows the changes in both direction and intensity as a vector endpoint projection.

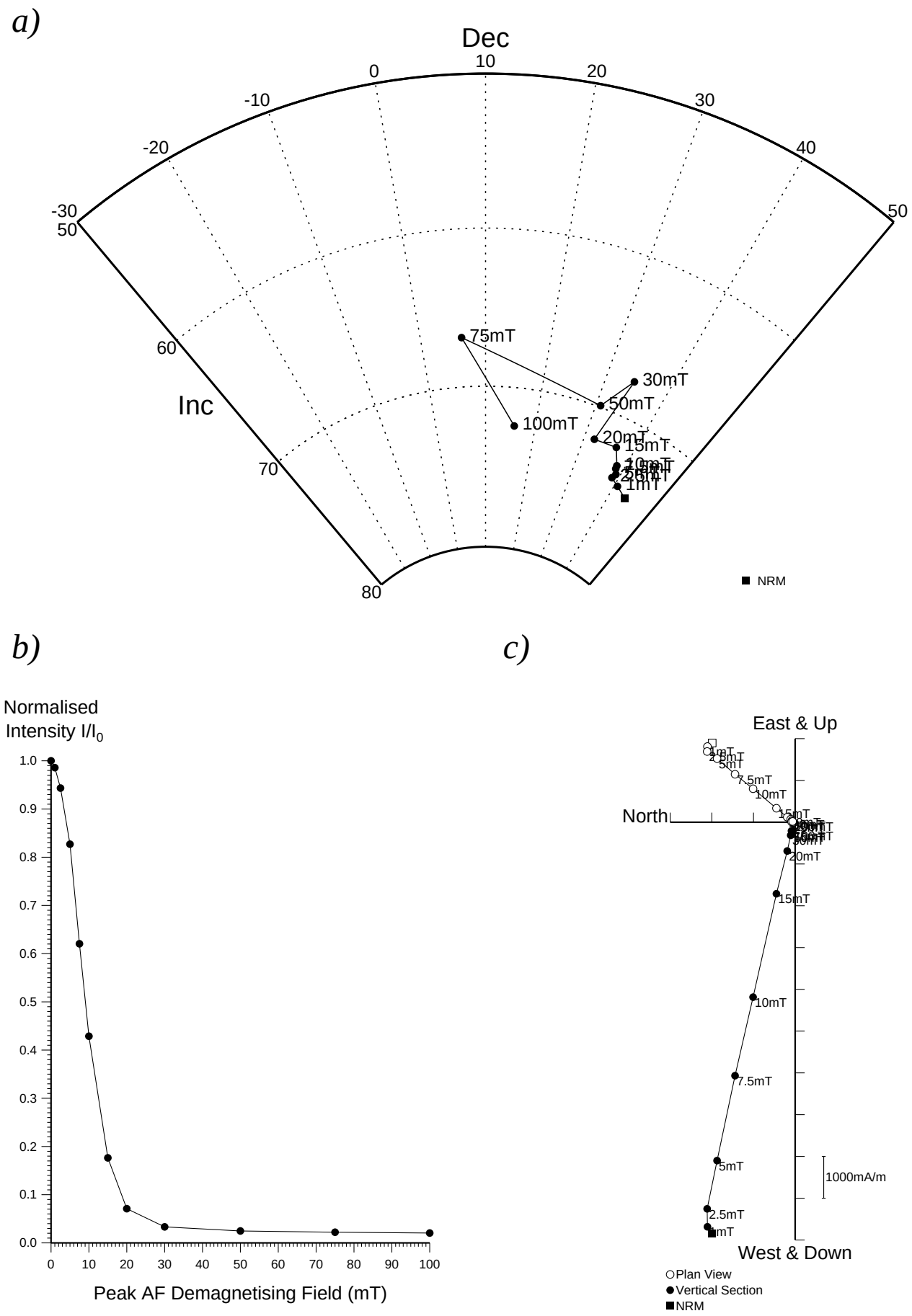

Figure 10: Stepwise AF demagnetisation of sample IM11. Diagram a) depicts the variation of the remanent direction as an equal area stereogram; b) shows the normalised change in remanence intensity as a function of the demagnetising field; c) shows the changes in both direction and intensity as a vector endpoint projection.

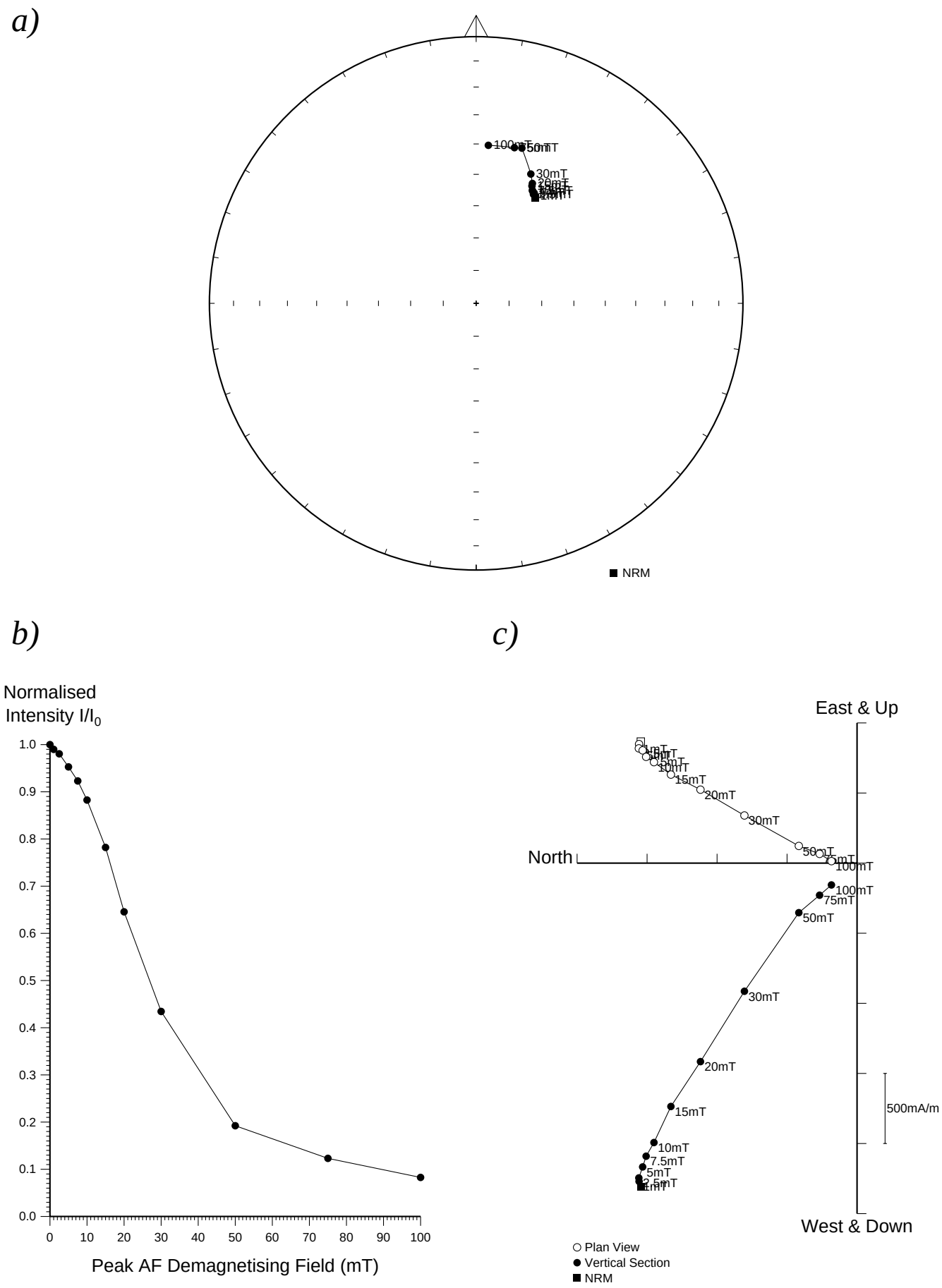

Figure 11: Stepwise AF demagnetisation of sample IM17. Diagram a) depicts the variation of the remanent direction as an equal area stereogram (declination increases clockwise, while inclination increases from zero at the equator to 90 degrees at the centre of the projection); b) shows the normalised change in remanence intensity as a function of the demagnetising field; c) shows the changes in both direction and intensity as a vector endpoint projection.

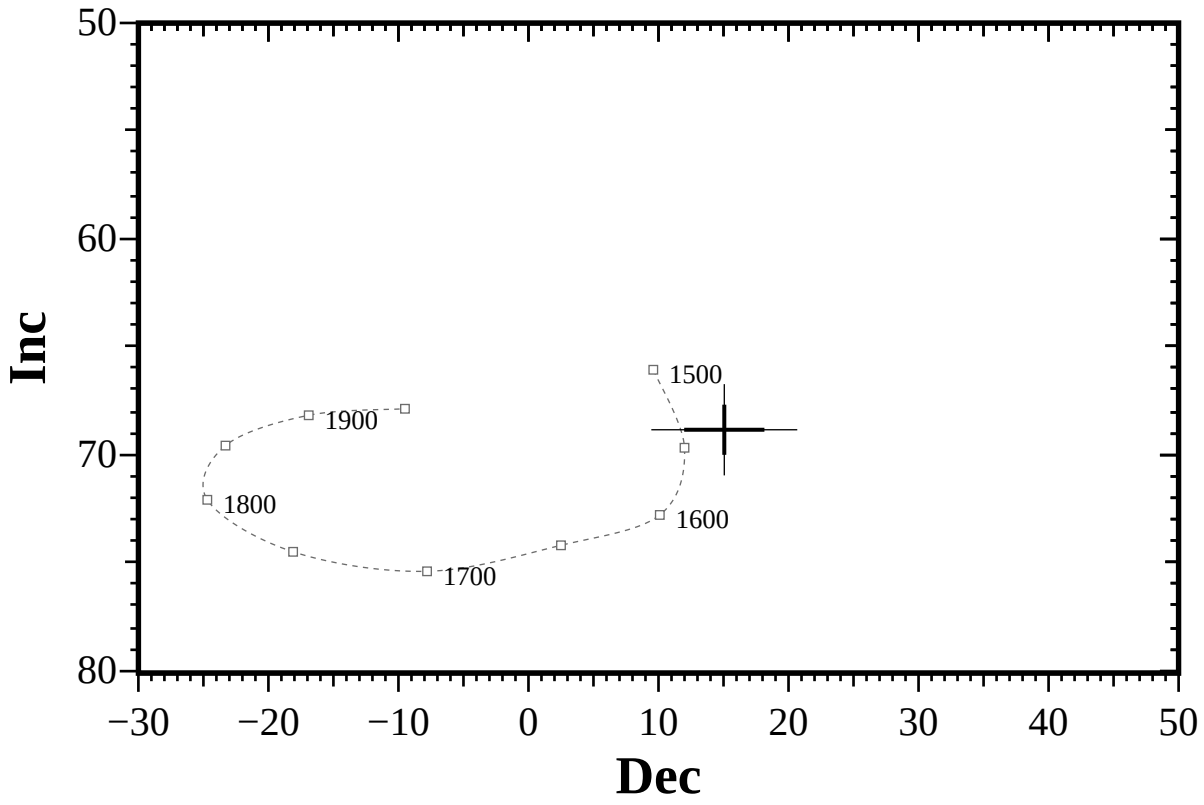

Figure 12: Comparison of the mean thermoremanent vector calculated from samples 01-06, 09-10, 12-16 and 18-21 from feature IM after partial demagnetisation with the UK master calibration curve. Thick error bar lines represent 63% confidence limits and narrow lines 95% confidence limits.

Historic England Research and the Historic Environment

We are the public body that looks after England's historic environment. We champion historic places, helping people understand, value and care for them.

A good understanding of the historic environment is fundamental to ensuring people appreciate and enjoy their heritage and provides the essential first step towards its effective protection.

Historic England works to improve care, understanding and public enjoyment of the historic environment. We undertake and sponsor authoritative research. We develop new approaches to interpreting and protecting heritage and provide high quality expert advice and training.

We make the results of our work available through the Historic England Research Report Series, and through journal publications and monographs. Our online magazine Historic England Research which appears twice a year, aims to keep our partners within and outside Historic England up-to-date with our projects and activities.

A full list of Research Reports, with abstracts and information on how to obtain copies, may be found on www.HistoricEngland.org.uk/researchreports

Some of these reports are interim reports, making the results of specialist investigations available in advance of full publication. They are not usually subject to external refereeing, and their conclusions may sometimes have to be modified in the light of information not available at the time of the investigation.

Where no final project report is available, you should consult the author before citing these reports in any publication. Opinions expressed in these reports are those of the author(s) and are not necessarily those of Historic England.

The Research Report Series incorporates reports by the expert teams within the Investigation& Analysis Division of the Heritage Protection Department of Historic England, alongside contributions from other parts of the organisation. It replaces the former Centre for Archaeology Reports Series, the Archaeological Investigation Report Series, the Architectural Investigation Report Series, and the Research Department Report Series

ISSN 2059-4453 (Online)